ACS OMEGA

Article

Cite This: ACS Omega 2019, 4, 12432−12437

http://pubs.acs.org/journal/acsodf

^{64}Cu-Labeled Ubiquitin for PET Imaging of CXCR4 Expression in Mouse Breast Tumor

Huiqiang Li,[†,‡] Xiaohui Zhang,[‡] Hsuan Yi Wu,[§] Lingyi Sun,[‡,∥] Yongyong Ma,[‡,∥] Junling Xu,[†] Qing Lin,*[,§] and Dexing Zeng*[,‡,∥]

[†]PET-CT Center, Department of Nuclear Medicine, Henan Provincial People's Hospital, Weiwu Road, No. 7, Jinshui District, Zhengzhou, Henan CN 450003, China

[‡]Molecular Imaging Laboratory, Department of Medicine, University of Pittsburgh, 3501 Fifth Avenue, Pittsburgh, Pennsylvania 15219, United States

[§]Department of Chemistry, State University of New York at Buffalo, 679 Natural Sciences Complex, Buffalo, New York 14260, United States

[∥]Department of Diagnostic Radiology, Oregon Health & Science University, 3181 S.W. Sam Jackson Park Rd., CRR210B, Portland, Oregon 97239, United States

Supporting Information

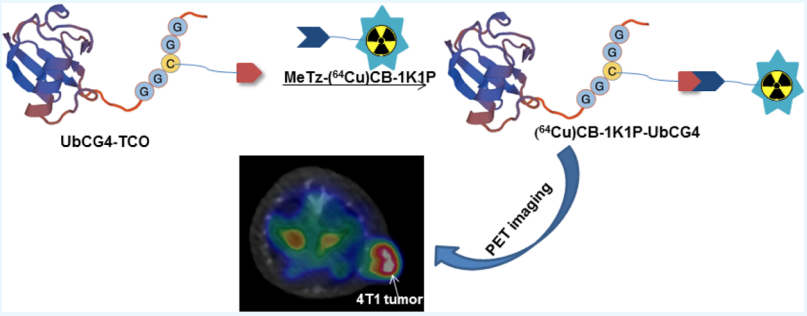

ABSTRACT: Ubiquitin has been recently identified as a chemokine receptor 4 (CXCR4) natural ligand, offering great potential for positron emission computed tomography (PET) imaging of CXCR4 expression. This study reports the preparation and evaluation of (^{64}Cu)-radiolabeled ubiquitin for CXCR4 imaging. The ubiquitin was first fused with a C-terminal GGCGG sequence, and the resulting recombinant ubiquitin derivative UbCG4 was then functionalized with the *trans*-cyclooctene (TCO) moiety via thiol−maleimide click reaction, followed by ^{64}Cu-radiolabeling through the TCO/Tz (tetrazine)-based Diels−Alder click reaction. In the prepared in vitro studies, the prepared (^{64}Cu)-UbCG4 showed significantly higher specific uptakes in the 4T1 breast cancer cells compared with the uptakes in the CXCR4-knockdown 4T1 cells. In the in vivo evaluation in the 4T1-xenograft mouse model, (^{64}Cu)-UbCG4 demonstrated a similar tumor uptake but much lower backgrounds compared with ^{64}Cu-labeled AMD3465. These results suggested that (^{64}Cu)-UbCG4 could serve as a potent PET tracer for the noninvasive imaging of CXCR4 expression in tumors.

1. INTRODUCTION

PET imaging is an attractive platform for noninvasive visualization, early detection, and potential therapy of diseases.[1] The detection of a given receptor on the cell surface is a major means to image the molecular and cellular processes.[2] CXCR4 has become one of the best studied chemokine receptors in the last decade because of its fundamental roles in numerous diseases such as cancer and HIV.[3] CXCR4 is a seven-transmembrane G protein-coupled receptor with the stromal cell-derived factor-1α (SDF-1α, also known as CXCL12) serving as its native ligand. The CXCR4/SDF-1α axis is important for normal development and hematopoiesis and plays pleiotropic roles in tumor metastasis, HIV entry, inflammatory response, and cell trafficking in autoimmune diseases.[4] Recently, CXCR4 was found to be overexpressed in at least 23 different hematopoietic, epithelial, and mesenchymal cancers.[5] The overexpression of CXCR4 in tumors usually correlates with tumor aggressiveness,[6,7] poor prognosis and survival,[8] increased risk of metastasis,[9] higher probability of recurrence, and resistance to chemotherapy.[10] Therefore, considerable efforts were made to visualize and quantify CXCR4 expression in tumors noninvasively using PET. A variety of radiolabeled CXCR4 antagonists have been developed, including small molecules, peptides, antibodies, pepducins, and nanoparticles.[11−14] These radiolabeled antagonists can detect CXCR4 expression in tumors, and some of

Received: March 11, 2019
Accepted: June 28, 2019
Published: July 22, 2019

DOI: 10.1021/acsomega.9b00678
ACS Omega 2019, 4, 12432−12437

Scheme 1. Schematic Illustration of Preparation of (^{64}Cu)CB-1K1P-UbCG4

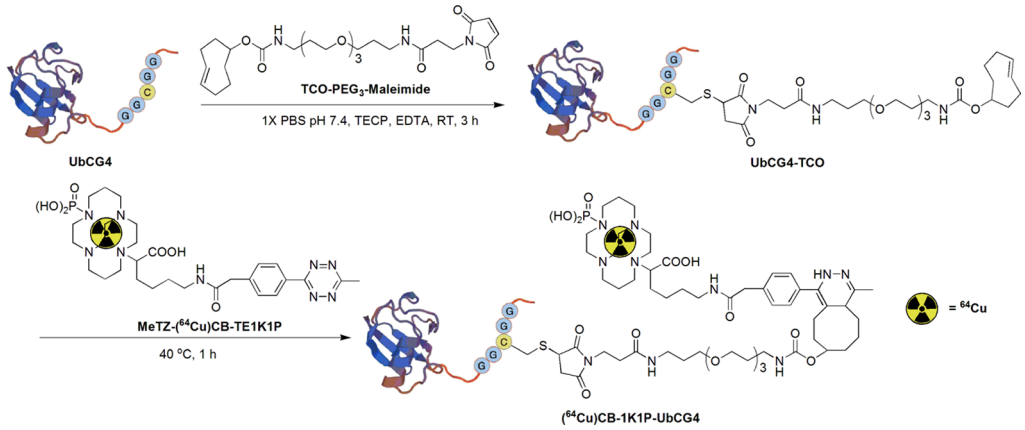

them have even entered into clinical trials. However, they also exhibited a number of drawbacks, including high accumulation in the liver, relatively low accumulation in CXCR4-positive tumors, binding to red blood cells, and lack of cross-reactivity between human/animal CXCR4 proteins.[12]

Ubiquitin, another ligand of CXCR4, is a highly conserved 76-amino acid residue protein covalently attached to substrate proteins via an isopeptide bond through a multistep enzymatic process that requires the activating E1, conjugating E2, and ligating E3 enzymes.[15] As a post-translational protein modifier in the cell, ubiquitin was also reported to act as an agonist of CXCR4 with strong affinity (K_d, 156 ± 27 nM)[16−18] when it is present outside the cell. Unlike its endogenous ligand SDF-1α, ubiquitin does not bind CXCR7, and its function as a CXCR4 agonist does not interfere with the productive cellular entry of HIV-1. Through binding to CXCR4, unanchored extracellular ubiquitin is involved in apoptosis, cell growth, immune modulation, and cancer progression.[16,18,19] Consequently, ubiquitin is capable of being a potential pharmaceutical agent to target CXCR4, and thus it is a logical choice for the development of highly specific CXCR4 radiotracers. Further, because of the observed cross-reactivity between human/animal CXCR4 proteins,[12] it is believed that the development of ubiquitin-based CXCR4-targeting PET tracers may greatly facilitate the clinical translation.

In this study, a novel ubiquitin-based CXCR4 targeting PET tracer [(^{64}Cu)CB-1K1P-UbCG4] was developed, which was prepared by first radiolabeling a new cross-bridged cyclam chelator (MeTz-CB-1K1P) with ^{64}Cu, followed by the conveniently bio-orthogonal Diels−Alder click reaction between methyl-tetrazine [MeTz-(^{64}Cu)CB-1K1P] and *trans*-cyclooctene (TCO-UbCG4) moieties (Scheme 1). The resulting (^{64}Cu)CB-1K1P-UbCG4 was then evaluated in vitro in the 4T1 breast cancer cells as well as in vivo in the mice bearing 4T1 xenografts. In addition, the biodistribution of (^{64}Cu)CB-1K1P-UbCG4 was also compared with those of (^{64}Cu)-AMD3465, a classic small molecule-based CXCR4 PET imaging tracer.[20]

2. RESULTS AND DISCUSSION

The upregulation of CXCR4 has been reported in many cancers, and the interaction with its endogenous ligand SDF-1 has been shown to play a pivotal role in tumor growth and metastasis. CXCR4 hence represents an attractive target for cancer imaging and/or therapeutic intervention. In general, CXCR4-specific imaging probes were prepared by functionalizing a small-molecule CXCR4 antagonist with a chelator or prosthetic group. Ubiquitin is a natural CXCR4 ligand and thus has been considered to be a logical choice for CXCR4-targeted imaging and/or therapy. In this study, the preparation and evaluation of the ^{64}Cu-labeled ubiquitin for noninvasive detection of CXCR4 expression in the mammary carcinoma 4T1 xenograft mouse model was described, including the preparation of UbCG4-TCO, ^{64}Cu-radiolabeling, in vitro cell binding, ex vivo biodistribution, and in vivo PET imaging in mice bearing CXCR4-overexpressed mouse mammary carcinoma 4T1 tumors.

2.1. Synthesis of UbCG4-TCO. With the rapid development of click reactions in chemical biology and bio-orthogonal ligations have emerged in the last decades for various biomedical applications, including the preparation of radiotracers for nuclear imaging and/or radionuclide therapy. Such conjugation reactions include the Cu-catalyzed azide−alkyne cycloaddition,[21] the strain-promoted azide−alkyne cycloaddition,[22] the inverse electron demand Diels−Alder reaction (IEDDA),[23] and the Staudinger ligation.[24] Compared with other reported metal-free click reactions, the IEDDA cycloaddition between TCO/Tz offers the highest reaction rate and thus has been used in the preparation of different radiotracers for nuclear imaging and radionuclide therapy.[25,26] Thus, a ubiquitin derivative UbCG4 was prepared as previously reported[27] by fusing the cysteine-contained pentapeptide sequence GG**C**GG at the C-terminus of ubiquitin. The thiol group on the cysteine side chain was sterically unhindered and thus could participate in a variety of nucleophilic reactions. Indeed, the cysteine thiol is generally considered to be the strongest nucleophile among all other amino acid side chains under physiological conditions (pH 7.4). It has been exploited in the development of many useful cysteine-specific bioconjugation reactions.[28,29] Then, the prepared UbCG4 protein was conjugated with a maleimide derivative containing a PEG3 chain and a TCO moiety in the presence of tris(2-carboxyethyl)-phosphine (TCEP). The reaction was monitored by fast protein liquid chromatography (FPLC). During the reaction, the pH of the solution was maintained at 6−7, which was crucial because the maleimide group could be hydrolyzed to a nonreactive maleamic acid when pH was greater than 8.[30] After incubation for 3 h, the mixture was subjected to dialysis using a dialysis bag with the molecular weight cutoff at 3.5 K. Mass spectrometry was used to confirm the success of the conjugation between UbCG4 and maleimido PEG3-TCO (MS expected: 11 830.1; MS observed: 11 829.5).

DOI: 10.1021/acsomega.9b00678
ACS Omega 2019, 4, 12432−12437

Further, FPLC analysis gave a yield of more than 98% using a Tz-decorated indicator (Tz-Cy5) (Figure S1), which also validated the high efficiency and quantitative labeling using the Tz/TCO click chemistry.

2.2. Radiochemistry. (^{64}Cu)CB-1K1P-UbCG4 was prepared via a two-step strategy: chelator MeTz-CB-1K1P was first radiolabeled with ^{64}Cu with good specific activity (1×10^3 mCi/μmol), and then the resulting MeTz-(^{64}Cu)CB-1K1P was ligated to ubiquitin derivative UbCG4-TCO via the bioorthogonal Diels–Alder click chemistry between the MeTz and TCO moieties. This two-step strategy offers the advantage of modular synthesis of radiotracers, which allows attaching different imaging moieties, such as MeTz-Cy7, MeTz-(^{68}Ga)-NOTA, and MeTz-(^{89}Zr)-DFO. Compared with other cross-bridged cyclam chelators (CB-TE2A and CB-1A1P), the recently reported cross-bridged cyclam chelator CB-1K1P could be radiolabeled with ^{64}Cu under mild conditions with high specific activity,[31] and therefore it was employed in this study. MeTz-CB-1K1P was radiolabeled with ^{64}Cu in ammonium acetate buffer (pH 8.2), and radioactive high-performance liquid chromatography (HPLC) was used to monitor the radiolabeling efficiency. Because the MeTz moiety hydrolyzes in the basic radiolabeling buffer, we monitored radiolabeling closely to minimize the hydrolysis of the MeTz moiety, and once the radiolabeling efficiency was more than 98%, the obtained MeTz-(^{64}Cu)CB-1K1P was immediately mixed with precursor UbCG4-TCO. The conjugation of MeTz-(^{64}Cu)CB-1K1P with UbCG4-TCO was performed at 40 °C, and the reaction was monitored by radio-FPLC. In any case where the conversion was lower than 95%, an appropriate desalting column could be used to remove residual MeTz-(^{64}Cu)CB-1K1P. The total radiosynthesis time was about 1.0 h, and the overall radiochemical yield was about 75 ± 2.8% (not decay-corrected). As determined by radio-FPLC (Figure 1), the radiopurity of (^{64}Cu)CB-1K1P-UbCG4 was more than 98%, and the specific activity was 1×10^3 mCi/μmol (37 GBq/μmol).

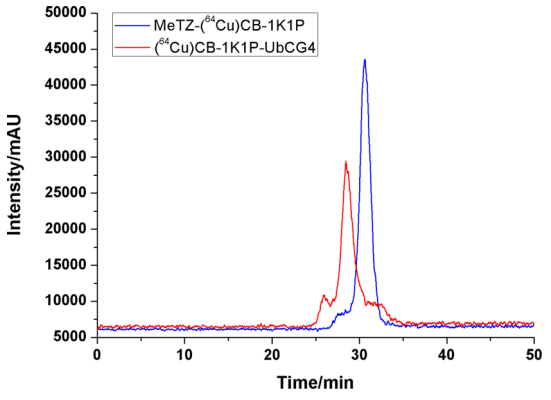

Figure 1. Radio-FPLC trace of MeTz-(^{64}Cu)CB-1K1P and (^{64}Cu)CB-1K1P-UbCG4.

2.3. In Vitro and in(ex) Vivo Evaluation. To estimate the binding effect of the prepared radiotracer, cell uptake studies were first performed. In the in vitro cell studies, the radiotracer (^{64}Cu)CB-1K1P-UbCG4 was incubated with CXCR4-expressing 4T1 cells and CXCR4-knockdown 4T1 cell lines, respectively, at 1 and 2 h time intervals (Figure 2). At 1 h incubation time point, its uptake by CXCR4-expressing 4T1 and CXCR4-knockdown 4T1 cells was 3.67 ± 0.63 and 0.74 ± 0.18, respectively. After subtracting the non-CXCR4-specific uptake, its CXCR4-specific uptake on 4T1 was 2.93 ± 0.49 at 1 h incubation time point. The different cell uptakes of (^{64}Cu)CB-1K1P-UbCG4 by CXCR4-expressing and CXCR4-knockdown cells demonstrated the specificity of the radiotracer. When the incubation time was extended to 2 h, its uptake on CXCR4-expressing 4T1 cells remained unchanged and that on CXCR4-knockdown, 4T1 cells just slightly increased, indicating that the cellular uptake of (^{64}Cu)CB-1K1P-UbCG4 was mediated by the CXCR4 receptor.

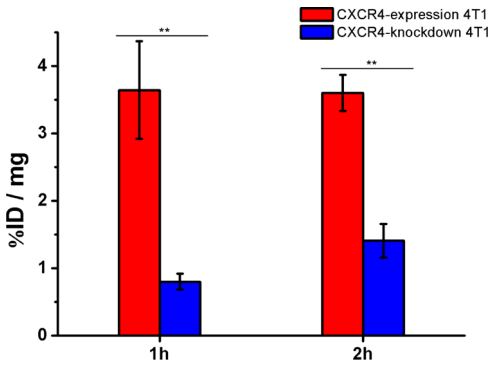

Figure 2. Cell uptake of (^{64}Cu)CB-1K1P-UbCG4 in CXCR4-expression and CXCR4-knockdown 4T1 cell lines at 1 and 2 h. Significant differences between groups are indicated with ** ($p < 0.005$, $n = 5$), and values represent the average ± standard deviations.

Encouraged by the promising in vitro results, (^{64}Cu)CB-1K1P-UbCG4 was further evaluated in a mouse xenograft model. Briefly, BALB/c mice (4–6 weeks old) bearing CXCR4-expressing 4T1 xenografts in the right front shoulder were injected with about 100 μCi of (^{64}Cu)CB-1K1P-UbCG4 after the tumor size reached about 100 mm, and then PET imaging was performed 1 and 2 h after injection. As shown in Figure 3, all xenografted tumors were clearly visible after injection with good tumor-to-background contrasts, and the tumor uptake value was (2.03 ± 0.13) % ID/g and (2.37 ± 0.11) % ID/g after 1 and 2 h, respectively, determined by quantitative analysis of the PET images. PET images obtained from (^{64}Cu)CB-1K1P-UbCG4 2 h after the injection were then compared with the ones obtained from the classic CXCR4 PET imaging probe (^{64}Cu)-AMD3465. Figure S2 shows that the tumor was not clearly visible, and the tumor uptake value was (0.78 ± 0.09) % ID/g, which was lower than that of (^{64}Cu)CB-1K1P-UbCG4, demonstrating the superi-

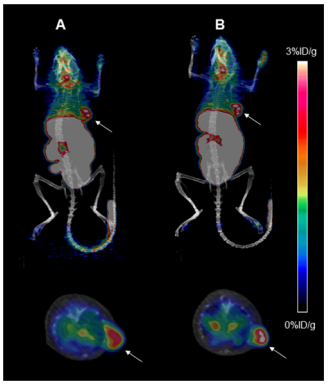

Figure 3. PET images of (^{64}Cu)CB-1K1P-UbCG4 post-injection 1 h (A) and 2 h (B); the white arrow indicates 4T1-expression tumor.

DOI: 10.1021/acsomega.9b00678
ACS Omega 2019, 4, 12432–12437

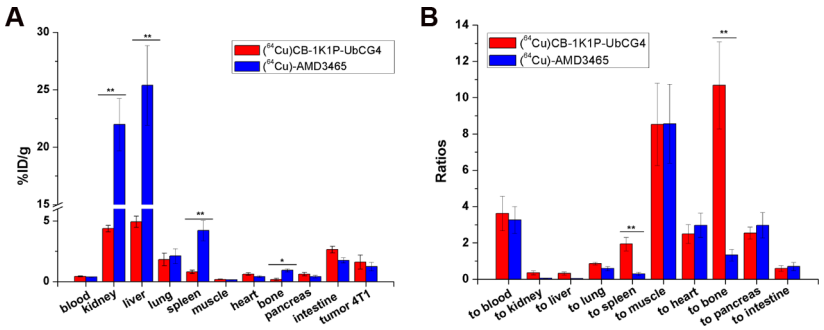

Figure 4. Biodistribution (A) and ratios of tumor to organs (B) of (^{64}Cu)CB-1K1P-UbCG4 and (^{64}Cu)-AMD3465 post-injection 2 h. Significant differences between groups are indicated with * ($p < 0.05$) or ** ($p < 0.005$). Data represent an average of six mice ± standard deviations.

ority of (^{64}Cu)CB-1K1P-UbCG4 over (^{64}Cu)-AMD3465. Besides the CXCR4-specific uptakes in tumors, the (^{64}Cu)CB-1K1P-UbCG4 also showed relatively high uptakes in the liver and kidneys, which was similar to that with other CXCR4-targeting PET tracers, such as (^{64}Cu)-AMD3465 and (^{64}Cu)-AMD3100.[20,32] The noticeable uptake in the liver and kidneys should not be attributed to CXCR4-specific binding because liver cells expressed only very limited CXCR4,[33] and other high-CXCR4-expressing organs such as spleen did not show such a high uptake of these tracers.

To further validate the use of (^{64}Cu)CB-1K1P-UbCG4, ex vivo biodistribution studies were then conducted to compare the tumor/nontumor ratios between the developed PET tracer and classic CXCR4 PET imaging probe (^{64}Cu)-AMD3465. The biodistribution results obtained from both radiotracers are shown in Figure 4. Compared with (^{64}Cu)-AMD3465, (^{64}Cu)CB-1K1P-UbCG4 showed a significantly lower accumulation in normal CXCR4-expressing tissues, such as spleen, bone marrow, liver, and kidneys, in which the nonspecific uptake could result in background staining,[34] and this was one of the major concerns related to the routine use of (^{64}Cu)-AMD3465.[12] In particular, Figure 4 reveals a higher uptake of (^{64}Cu)CB-1K1P-UbCG4 in the CXCR4-expressing tumor (1.61 ± 0.58) compared with (^{64}Cu)-AMD3465 (1.24 ± 0.34), although the difference was not statistically significant. Compared with the small-molecule CXCR4 ligand (AMD3465), the peptide tracer showed a similar uptake in blood but significantly reduced hepatic and renal uptakes ($P < 0.005$, for both organs), which is highly desired for PET imaging of abdominal cancers. (^{64}Cu)CB-1K1P-UbCG4 also demonstrated a significantly higher ratio of the tumor to muscle (8.53 ± 2.26), tumor to spleen (1.94 ± 0.37), and tumor to bone marrow (10.68 ± 2.40) compared with (^{64}Cu)-AMD3465, suggesting good signal-to-noise ratios of (^{64}Cu)CB-1K1P-UbCG4. The hydrophilic chelates could promote fast renal clearance and reduce the nonspecific uptake due to the reduced retention in the nontumorous tissue.[11] Hence, the significant differences observed between (^{64}Cu)CB-1K1P-UbCG4 and (^{64}Cu)-AMD3465 might be attributed to the better hydrophilicity of the CB-1K1P-UbCG4 conjugate. Further, in addition to CXCR4, AMD3465 might also bind to CXCR7,[35] which was expressed in bone marrow and spleen.[36] In contrast, the ubiquitin was not a ligand of CXCR7,[16] which probably resulted in the radiouptake reduction in the bone marrow and spleen. In summary, the ex vivo biodistribution results were consistent with those obtained from PET images, further suggesting that the developed (^{64}Cu)CB-1K1P-UbCG4 could be potentially useful for in vivo CXCR4 imaging.

3. CONCLUSIONS

In this study, the recombinant ubiquitin protein UbCG4 was developed as a novel CXCR4-targeted PET radiotracer [(^{64}Cu)CB-1K1P-UbCG4], which was radiolabeled with ^{64}Cu through the Diels–Alder click chemistry between MeTz and TCO. The prepared (^{64}Cu)CB-1K1P-UbCG4 was then evaluated in 4T1 cell lines and the 4T1 tumor xenograft mouse model. Both in vitro and in(ex) vivo data demonstrated that (^{64}Cu)CB-1K1P-UbCG4 was selective and specific in binding with CXCR4 receptors in 4T1 tumors, which naturally express the receptor. Compared with the classic small-molecule CXCR4 imaging radiotracer (^{64}Cu)-AMD3465, (^{64}Cu)CB-1K1P-UbCG4 showed similar tumor uptakes but much lower accumulation in normal tissues and organs, especially in the kidney, liver, and spleen. Taken together, the results warranted further development of (^{64}Cu)CB-1K1P-UbCG4 as a PET agent for noninvasive PET imaging of CXCR4 expression in mice.

4. EXPERIMENTAL SECTION

4.1. Materials and Chemical Reagents. The reagents were purchased from commercial sources and used without further purification. The chemical purity of synthesized compounds was determined by the reverse-phase HPLC system, using an LC Workstation consisting of a Waters 1525 binary HPLC pump (MA, USA) and Waters 2998 photodiode array detector with wavelengths set at 280 nm. Chromatographic separation was performed on a Luna C18 ODS2 analytical column (5 μm, 150 × 4.6 mm inner diameter, Phenomenex, CA, USA). Waters LCT-Premier XE LC–MS station (MA, USA) was used to determine the molecular weight of the synthesized compounds.

4.2. Synthesis of Chelator MeTz-CB-TE1K1P. CB-TE1K1P was synthesized by the previously reported method.[31] DIEA (30 μmol) was added to a solution of CB-TE1K1P (5 μmol) and MeTz-NHS (15 μmol) in 500 μL of DMSO. After the resulting mixture was stirred for 1 h at room temperature, more than 96% yield was obtained based on HPLC analysis. The residue was purified using preparative HPLC and then obtained as a red powder. High-res ESI-MS: observed, m/z $(M + H)^+$, 662.3562; calcd exact mass m/z $(M + H)^+$, 662.3543.

4.3. Synthesis of Precursor UbCG4-TCO. UbCG4 was prepared by the previously reported method.[27] TCEP (500 nmol, 50 equiv) was added to a solution of UbCG4 (10 nmol, 1 equiv) in 200 μL of phosphate-buffered saline (1×, pH 7.4). The resulting reaction mixture was stirred for 30 min at room temperature. Then, TCO-PEG3-maleimide (100 nmol, 10 equiv) and ethylenediaminetetraacetic acid (5 mM) were

DOI: 10.1021/acsomega.9b00678
ACS Omega 2019, 4, 12432–12437

added and stirred for 3 h at room temperature. The pH value of the reaction solution was kept at 6−7. After the reaction was completed, the reaction mixture was purified by the dialysis method (molecular weight 3.5 K).

4.4. Radiochemistry. (^{64}Cu)−$CuCl_2$ was purchased from the Washington University (St. Louis, MO). (^{64}Cu)CB-1K1P-UbCG4 was prepared by using a two-step strategy. First, 2 nmol MeTz-CB-1K1P was added to 2 mCi (74 MBq) of (^{64}Cu)−$CuCl_2$ buffered with 200 μL 0.1 M ammonium acetate (pH, 8.2) and heated at 90 °C for 30 min. The resulting mixture was monitored on radioactive HPLC (-Agilent) using a C-18 column (Luna, 5 μm, 150 × 4.60 mm). MeTz-(^{64}Cu)CB-1K1P was then mixed with 4 nmol UbCG4-TCO at 40 °C for 30 min and monitored by radioactive FPLC (radio-FPLC) using a Superose 12 10/300 GL column.

4.5. Cell Cultures. The mouse mammary carcinoma CXCR4-expression and CXCR4-knockdown 4T1 cell lines were kindly provided by Dr. Yongjian Liu at Washington University in St. Louis, and the expression levels of these two cell lines were the same as his previous report.[14] The two cell lines were cultured in SIGMA Dulbecco's modified Eagle medium treated with 10% sterile filtered fetal bovine serum and 1% antibiotic penicillin−streptomycin−glutamine. The cell cultures were maintained at 37 °C in a 5% CO_2 controlled atmosphere with subculturing done every 3−4 days. The trypan-blue exclusion test was used for cell counting.

4.6. Cell Uptake Study. The cell study was performed to determine the binding affinity of (^{64}Cu)CB-1K1P-UbCG4 in CXCR4-expression and knock-down 4T1 cells. Cells were seeded in 24 well plates (10^5 cells per well) 24 h ahead of the experiment. Before the experiment, cells were washed with 1 mL Hanks balanced salt solution (HBSS) twice to remove the growth medium, and 0.5 mL binding medium (HBSS with 0.1% BSA) was added to each well. (^{64}Cu)CB-1K1P-UbCG4 (0.2 MBq) was added to the wells and then samples were incubated for 1 and 2 h at 37 °C. After incubation, the radioactive medium was removed. Cell pellets were rinsed twice with HBSS (1 mL) and dissolved in 1% sodium dodecyl sulfate solution. The radioactivity in each cell lysate sample was measured in a γ-counter. The protein content of each cell lysate sample was determined by the Pierce BCA Protein Assay Kit. The measured percentage dose associated with each cell lysate sample was normalized to the amount of cell protein present (ID %/mg).

4.7. Animal Model. All animal experiments were conducted under a protocol approved by the University of Pittsburgh Institutional Animal Care and Use Committee. Normal athymic BALB/c mice (16−22 g, 4−6 weeks old, n = 3) were obtained from Taconic. For implantation, 4T1 cells were harvested, and 10^6 cells in 200 μL mixture of phosphate-buffer saline and matrigel (v/v, 1/1) were inoculated subcutaneously on the right shoulder of mice. After an average time of 1.5 weeks, tumor size was large enough (about 100 mm) for the biodistribution and PET imaging studies.

4.8. Biodistribution Study. 4T1 expression xenograft tumor-bearing BALB/c mice (n = 6) were injected intravenously with (^{64}Cu)CB-1K1P-UbCG4 (3.7 MBq). The tumor-bearing mice were sacrificed by isoflurane anesthesia at 1.5 h after injection. Subsequently, the tissues and organs of interest were harvested, weighed, and radioactivity was counted using a γ-counter. Biodistribution data were given as the percentage injected dose per gram of tissues or organs (% ID/g) and was determined by decay correction for each sample normalized to a standard of known weight, which was representative of the injected dose.

4.9. Small-Animal PET/CT Imaging. For PET images, 4T1 expression xenograft tumor-bearing mcie (n = 3) were injected intravenously with (^{64}Cu)CB-1K1P-UbCG4 (3.7 MBq). Static images were acquired for a period of 15 min using a small-animal Inveon PET/CT scanner (Siemens Medical Solution) at 1.5 h post-injection.

4.10. Statistical Analysis. Statistical analysis was performed using the two-sided unpaired student's t-test in GraphPad 6. Probability (p) values less than 0.05 were considered statistically significant.

■ ASSOCIATED CONTENT

Supporting Information

The Supporting Information is available free of charge on the ACS Publications website at DOI: 10.1021/acsomega.9b00678.

FPLC traces of Tz-Cy5 and UbCG4-TCO and PET images of (^{64}Cu)-AMD3465 post-injection 2 h (PDF)

■ AUTHOR INFORMATION

Corresponding Authors

*E-mail: qinglin@buffalo.edu (Q.L.).
*E-mail: zengd@ohsu.edu (D.Z.).

ORCID

Huiqiang Li: 0000-0003-1375-9908
Lingyi Sun: 0000-0003-2111-8764
Qing Lin: 0000-0002-9196-5718
Dexing Zeng: 0000-0003-4948-5275

Author Contributions

H.L. and X.Z. contributed equally to this work.

Notes

The authors declare no competing financial interest.

■ ACKNOWLEDGMENTS

We gratefully acknowledge support for this work from the National Institute of Biomedical Imaging and Bioengineering grant R21-EB020737 and the American Cancer Society Research Scholar ACS-RSG-17-004-01-CCE. We thank Dr. Yongjian Liu at Washington University in St. Louis for generously sharing the CXCR4-expression and CXCR4-knockdown 4T1 cell lines. Preclinical PET/CT imaging is supported in part by P30CA047904 (UPCI CCSG).

■ REFERENCES

(1) Mankoff, D. A. A definition of molecular imaging. *J. Nucl. Med.* **2007**, *48*, 18N−21N.

(2) James, M. L.; Gambhir, S. S. A molecular imaging primer: modalities, imaging agents and applications. *Physiol. Rev.* **2012**, *92*, 897−965.

(3) Horuk, R. Chemokine receptors. *Cytokine Growth Factor Rev.* **2001**, *12*, 313−335.

(4) Domanska, U. M.; Kruizinga, R. C.; Nagengast, W. B.; Timmer-Bosscha, H.; Huls, G.; de Vries, E. G. E.; Walenkamp, A. M. E. A review on CXCR4/CXCL12 axis in oncology: no place to hide. *Eur. J. Cancer* **2013**, *49*, 219−230.

(5) Balkwill, F. The significance of cancer cell expression of the chemokine receptor CXCR4. *Semin. Cancer Biol.* **2004**, *14*, 171−179.

(6) Lee, H. J.; Kim, S. W.; Li, S.; Yun, H. J.; Song, S.; Kim, S.; Jo, D. Y. Chemokine receptor CXCR4 expression, function, and clinical implications in gastric cancer. *Int. J. Oncol.* **2009**, *34*, 473−480.

DOI: 10.1021/acsomega.9b00678
ACS Omega 2019, 4, 12432−12437

(7) Wagner, P. L.; Moo, T.-A.; Arora, N.; Liu, Y.-F.; Zarnegar, R.; Scognamiglio, T.; Fahey, T. J., 3rd. The chemokine receptors CXCR4 and CCR7 are associated with tumor size and pathologic indicators of tumor aggressiveness in papillary thyroid carcinoma. *Ann. Surg. Oncol.* **2008**, *15*, 2833−2841.
(8) Liu, Y.; Ji, R.; Li, J.; Gu, Q.; Zhao, X.; Sun, T.; Wang, J.; Li, J.; Du, Q.; Sun, B. Correlation effect of EGFR and CXCR4 and CCR7 chemokine receptors in predicting breast cancer metastasis and prognosis. *J. Exp. Clin. Cancer Res.* **2010**, *29*, 16.
(9) Cabioglu, N.; Sahin, A. A.; Morandi, P.; Meric-Bernstam, F.; Islam, R.; Lin, H. Y.; Bucana, C. D.; Gonzalez-Angulo, A. M.; Hortobagyi, G. N.; Cristofanilli, M. Chemokine receptors in advanced breast cancer: different expression in metastatic disease sites with diagnostic and therapeutic implications. *Ann. Oncol.* **2009**, *20*, 1013−1019.
(10) Ander, F.; Xia, W. Y.; Conforti, R.; Wei, Y. K.; Boulet, T.; Tomasic, G.; Spielmann, M.; Zoubir, M.; Berrada, N.; Arriagada, R.; Hortobagyi, G. N.; Hung, M.-C.; Pusztai, L.; Delaloge, S.; Michiels, S.; Cristofanilli, M. CXCR4 expression in early breast cancer and risk of distance recurrence. *Oncologist* **2009**, *14*, 1182−1188.
(11) Kuil, J.; Buckle, T.; van Leeuwen, F. W. B. Imaging agents for the chemokine receptor 4 (CXCR4). *Chem. Soc. Rev.* **2012**, *41*, 5239−5261.
(12) Weiss, I. D.; Jacobson, O. Molecular imaging of chemokine receptor CXCR4. *Theranostics* **2013**, *3*, 76−84.
(13) Chen, K.; Chen, X. Design and development of molecular imaging probes. *Curr. Top. Med. Chem.* **2010**, *10*, 1227−1236.
(14) Zhao, Y.; Detering, L.; Sultan, D.; Cooper, M. L.; You, M.; Cho, S.; Meier, S. L.; Luehmann, H.; Sun, G.; Rettig, M.; Dehdashti, F.; Wooley, K. L.; Dipersio, J. F.; Liu, Y. Gold nanoclusters doped with ^{64}Cu for CXCR4 positron emission tomography imaging of breast cancer and metastasis. *ACS Nano* **2016**, *10*, 5959−5970.
(15) Kleiger, G.; Mayor, T. Perilous journey: a tour of the ubiquitin-proteasome system. *Trends Cell Biol.* **2014**, *24*, 352−359.
(16) Saini, V.; Staren, D. M.; Ziarek, J. J.; Nashaat, Z. N.; Campbell, E. M.; Volkman, B. F.; Marchese, A.; Majetschak, M. The CXC chemokine receptor 4 ligands ubiquitin and stromal cell-derived factor-1α function through distinct receptor interaction. *J. Biol. Chem.* **2011**, *286*, 33466−33477.
(17) Saini, V.; Romero, J.; Marchese, A.; Majetschak, M. Ubiquitin receptor binding and signaling in primary human leukocytes. *Commun. Integr. Biol.* **2010**, *3*, 608−610.
(18) Saini, V.; Marchese, A.; Majetschak, M. CXC chemokine receptor 4 is a cell surface receptor for extracellular ubiquitin. *J. Bio. Chem.* **2010**, *285*, 15566−15576.
(19) Yan, L.; Cai, Q.; Xu, Y. The ubiquitin-CXCR4 axis plays an important role in acute lung infection-enhanced lung tumor metastasis. *Clin. Cancer Res.* **2013**, *19*, 4706−4716.
(20) De Silva, R. A.; Peyre, K.; Pullambhatla, M.; Fox, J. J.; Pomper, M. G.; Nimmagadda, S. Imaing CXCR4 expression in human cancer xenografts: evaluation of monocyclam 64Cu-AMD3465. *J. Nucl. Med.* **2011**, *52*, 986−993.
(21) Thirumurugan, P.; Matosiuk, D.; Jozwiak, K. Click chemistry for drug development and diverse chemical-biology applications. *Chem. Rev.* **2013**, *113*, 4905−4979.
(22) Campbell-Verduyn, L. S.; Mirfeizi, L.; Schoonen, A. K.; Dierckx, R. A.; Elsinga, P. H.; Feringa, B. L. Strain-promoted copper free "click" chemistry for 18F radiolabeling of bombesin. *Angew. Chem., Int. Ed.* **2011**, *50*, 11117−11120.
(23) Reiner, T.; Zeglis, B. M. The inverse electron demand Diels-Alder click reaction in radiochemistry. *J. Labelled Compd. Radiopharm.* **2014**, *57*, 285−290.
(24) Schilling, C. I.; Jung, N.; Biskup, M.; Schepers, U.; Bräse, S. Bioconjugation via azide-Staudinger ligation: an overview. *Chem. Soc. Rev.* **2011**, *40*, 4840−4847.
(25) Selvaraj, R.; Giglio, B.; Liu, S.; Wang, H.; Wang, M.; Yuan, H.; Chintala, S. R.; Yap, L.-P.; Conti, P. S.; Fox, J. M.; Li, Z. Improved metabolic stability for 18F PET probes rapidly constructed via tetrazine *trans*-cyclooctene ligation. *Bioconjugate Chem.* **2015**, *26*, 435−442.
(26) Meyer, J.-P.; Tully, K. M.; Jackson, J.; Dilling, T. R.; Reiner, T.; Lewis, J. S. Bioorthogonal masking of circulating antibody-TCO groups using tetrazine-functionalized dextran polymer. *Bioconjugate Chem.* **2018**, *29*, 538−545.
(27) Ramil, C. P.; An, P.; Yu, Z.; Lin, Q. Sequence-specific 2-cyanobenzothiazole ligation. *J. Am. Chem. Soc.* **2016**, *138*, 5499−5502.
(28) Gianatassio, R.; Lopchuk, J. M.; Wang, J.; Pan, C.-M.; Malins, L. R.; Prieto, L.; Brandt, T. A.; Collins, M. R.; Gallego, G. M.; Sach, N. W.; Spangler, J. E.; Zhu, H.; Zhu, J.; Baran, P. S. Strain Release Amination. *Science* **2016**, *351*, 241−246.
(29) Vinogradova, E. V.; Zhang, C.; Spokoyny, A. M.; Pentelute, B. L.; Buchwald, S. L. Organometallic palladium reagents for cysteine bioconjugation. *Nature* **2015**, *526*, 687−691.
(30) Veronese, F. M. Peptide and protein PEGylation. *Biomaterials* **2001**, *22*, 405−417.
(31) Zeng, D.; Ouyang, Q.; Cai, Z.; Xie, X.-Q.; Anderson, C. J. New cross-bridged cyclam derivative CB-TE1K1P, an improved bifunctional chelator for copper radionuclides. *Chem. Commun.* **2014**, *50*, 43−45.
(32) Jacobson, O.; Weiss, I. D.; Szajek, L.; Farber, J. M.; Kiesewetter, D. O. 64Cu-AMD3100—a novel imaging agent for targeting chemokine receptor CXCR4. *Bioorg. Med. Chem.* **2009**, *17*, 1486−1493.
(33) Li, W.; Gomez, E.; Zhang, Z. Immunohistochemical expression of stromal cell-derived factor-1 (SDF-1) and CXCR4 ligand receptor system in hepatocellular carcinoma. *J. Exp. Clin. Cancer Res.* **2007**, *26*, 527−533.
(34) Buckle, T.; Van den Berg, N. S.; Kuil, J.; Bunschoten, A.; Oldenburg, J.; Borowsky, A. D.; Wesseling, J.; Masada, R.; Oishi, S.; Fujiii, N.; Van Leeuwen, F. W. B. Non-invasive longitudinal imaging of tumor progression using an 111Indium labeled CXCR4 peptied antagonist. *Am. J. Nucl. Med. Mol. Imaging* **2012**, *2*, 99−109.
(35) Hartimath, S. V.; Khayum, M. A.; van Waarde, A.; Dierckx, R. A. J. O.; De Vries, E. F. J. N-[11C]Methyl-AMD3465 PET as a tool for in vivo measuremnet of chemokine receptor 4 (CXCR4) occupancy by therapeutic drugs. *Mol. Imaging Biol.* **2017**, *19*, 570−577.
(36) Sánchez-Martín, L.; Paloma, S.-M.; Carlos, C. CXCR7 impact on CXCL12 biology and disease. *Trends Mol. Med.* **2013**, *19*, 12−22.

DOI: 10.1021/acsomega.9b00678
ACS Omega 2019, 4, 12432−12437